



ELSEVIER

International Journal of Mass Spectrometry 202 (2000) 161–174



# “Proton-transport” catalysis in the gas phase. Keto-enol isomerization of ionized acetaldehyde

G. van der Rest\*, H. Nedev, J. Chamot-Rooke, P. Mourgues, T.B. McMahon, H.E. Audier

*Laboratoire des Mécanismes Réactionnels, UMR CNRS 7651, Ecole Polytechnique, F-91128, Palaiseau, France*

Received 24 March 2000; accepted 28 March 2000

## Abstract

Fourier transform ion cyclotron resonance experiments show that a variety of molecules catalyze the hydrogen transfer which converts ionized acetaldehyde  $\text{CH}_3\text{CHO}^+$  **1** to its vinyl alcohol counterpart  $\text{CH}_2\text{CHOH}^+$  **2**. Each of these ions has been characterized by its specific bimolecular reactions with selected reactants. Calculations show that two pathways, for which the rate determining barriers have almost the same energy, are feasible. The first transition state involves a direct catalyzed 1,3-H transfer, while the second involves two successive 1,2-H transfers. A detailed experimental study, using methanol as a catalyst as well as labeled reactants, indicates that only the first pathway operates in the isomerization process. The different steps of these two independent pathways were elucidated. The first begins with the formation of a highly stabilized complex **3**, involving a two-center-three-electron interaction between the two oxygen atoms and an interaction between a hydrogen of the methyl group of **1** and the oxygen of methanol. This complex isomerizes into a complex **4**, which in turn gives the complex **5**, via a transition state located  $6.3 \text{ kcal mol}^{-1}$  below the energy of the reactants. This complex **5** corresponds to ionized vinyl alcohol hydrogen bonded to the oxygen of methanol, which dissociates to yield ion **2**. The second pathway begins with the interaction between the hydrogen of the CHO group and the oxygen of methanol and gives the complexes **6** and then **7**, which correspond to protonated methanol hydrogen bonded to a  $\text{CH}_3\text{CO}^\cdot$  radical. Dissociation of **7** to give protonated methanol is favoured with respect to further isomerization leading to ionized vinyl alcohol. Compared to the unimolecular conversion between energetic ions **1** and **2**, which can occur either by a direct 1,3-H transfer or by a double 1,2-H transfer, the reaction of **1** with methanol catalyzes the first pathway while inhibiting the second one. In the case studied, catalysis is perhaps better described as a hydrogen atom transport. (Int J Mass Spectrom 202 (2000) 161–174) © 2000 Elsevier Science B.V.

*Keywords:* Fourier transform ion cyclotron resonance; Keto-enol isomerization; Acetaldehyde; “Proton-transport” catalysis

## 1. Introduction

In solution, keto-enol isomerization is facile and is well known to be a bimolecular (or higher order) process [1]. In the gas phase, the unimolecular isomerization of an ionized aldehyde or ketone into its enolic counterpart

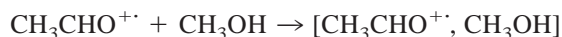
(which is generally much more stable [2]) is difficult [3] since the reaction involves a high energy barrier [4]. However, such processes can be induced by an ion–molecule interaction.

The reaction between an ion and a neutral molecule in the gas phase yields an encounter complex in which reactions can take place. Among these reactions, the neutral molecule can catalyze the isomer-

\* Corresponding author.

ization of the ion via a process generally described as “H<sup>+</sup> transport” [5]. It is important to study this process in order to open new perspectives for the interpretation of ion–molecule reactions as well as for reactions within complexes. For instance, it has been shown both by experiment [6] and by calculation [7] that one molecule of water catalyzes the 1,2-H shift that converts ionized methanol CH<sub>3</sub>OH<sup>+</sup> into its more stable isomer, the  $\alpha$ -dystonic ion CH<sub>2</sub>OH<sub>2</sub><sup>+</sup>. The mechanism of this reaction has been clearly established [6,7] while a significant number of other 1,2-H<sup>+</sup> transports have been described [8–10]. The same phenomenon has also been evidenced in anion chemistry where acid-catalyzed isomerizations within complexes are well known [11].

Appropriate neutral molecules catalyze 1,3-H transfers from oxygen to oxygen in ROCH<sub>2</sub>O(H)R<sup>+</sup> (R = H, CH<sub>3</sub>) ions [12–14]. Several catalyzed keto-



(1)

We report a detailed study of the reaction depicted in Eq. (1) which represents, at first sight, the simplest keto-enol isomerization in the gas phase. Experimental studies (in particular, kinetic energy release mea-

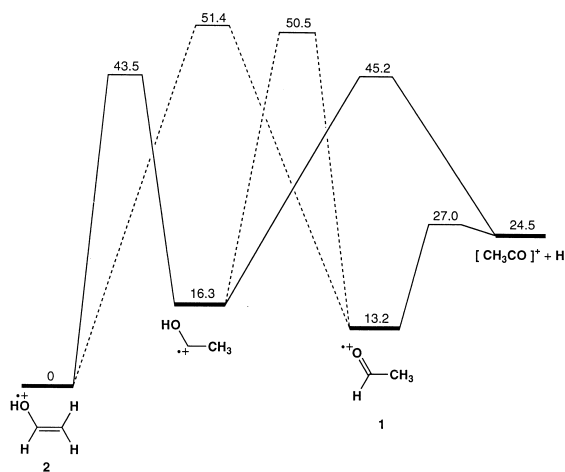


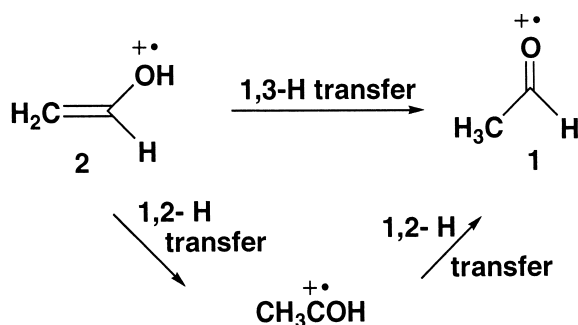
Fig. 1. Potential energy profile (kcal mol<sup>-1</sup>) for the unimolecular pathways connecting ionized acetaldehyde **1** and its enol isomer **2** (adapted from [4]).

enol tautomerism reactions have been proposed [15]. For instance water can convert ionized cyclohexadienone into ionized phenol [16]. Further, we have shown that appropriate molecules isomerize the H<sub>3</sub>COC(O)CH<sub>2</sub>CO<sup>+</sup> cation into its enol isomer [17], and we have also proposed that methanol catalyzes the 1,3-H transfer that converts ionized acetaldehyde into the more stable enol form [Eq. (1)] [17,18]. Trikoupi and Terlouw [19] have shown recently that, in the ion source of a mass spectrometer, the same phenomenon occurs with ionized acetone. However, in none of these 1,3-H transfer studies, the mechanism of the isomerization has been studied. Therefore, the first questions of interest are: how does the catalyst influence the mechanism, how many molecules of catalyst operate in the process and which molecules are efficient in performing this catalysis?

Measurements) show that the metastable CH<sub>3</sub>CHO<sup>++</sup> (*m/z* 44) radical cation **1** does not spontaneously isomerize to its more stable enol isomer CH<sub>2</sub>CHOH<sup>++</sup> **2** [3] prior to loss of H<sup>•</sup> (the principal dissociation pathway). In contrast, ion **2** may isomerize to CH<sub>3</sub>COH<sup>+</sup> and subsequently to **1** prior to this dissociation [3,4]. Calculations indicate that **1** and **2** are separated by substantial energy barriers [4] and that high energy ions **1** and **2** are connected by two pathways very close in energy (Fig. 1); the first involves a direct 1,3-H transfer and the second a double 1,2-H transfer (Scheme 1) [4]. Therefore, the second question of interest is to know if the pathways connecting ions **1** and **2** are the same in the unimolecular reaction and in the catalyzed process.

## 2. Experimental

The bimolecular reactions of ions **1** and **2** were examined in a Bruker CMS-47X Fourier Transform ion cyclotron resonance (FTICR) mass spectrometer



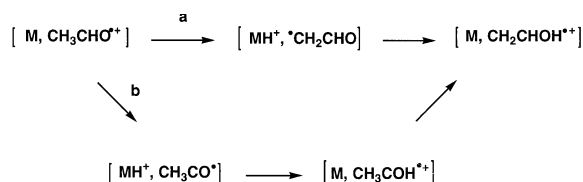
equipped with an external ion source [20] and an infinity cell [21]. The neutral reactants were introduced into the cell through a leak valve at a pressure of  $1 \times 10^{-8}$ – $4 \times 10^{-8}$  mbar (depending on the experiment) and then diluted with argon to give a total pressure of  $2 \times 10^{-7}$  mbar. Where appropriate, neutral reactant was introduced by means of a piezoelectric pulsed valve.

Ion–molecule reactions were examined after isolation and thermalization of the reactant ions formed in the external ion source. After transfer into the cell, the ion of interest was first isolated by radio frequency (rf) ejection of all unwanted ions. After a 1.5 s delay (usually sufficient to thermalize the ions by successive collisions with argon) the isolation procedure was repeated by the use of low-voltage single rf pulses (soft shots) at the resonance frequencies of the product ions formed during the relaxation time.

The efficiencies of the reactions are reported as the ratio of the experimental rate constant to the calculated collision rate constant according to Su and Chesnavich [22].

Labeled acetaldehydes and methanols were obtained commercially (Aldrich). Ion **2** was generated by fragmentation of ionized cyclobutanol.

The GAUSSIAN94 program package was used for calculations [23] to determine the different key structures on the potential energy profile. The geometries were optimized at the UMP2/6-31G\*\* level of theory [24]. Diagonalization of the computed Hessian was performed in order to confirm that the structures were minima or transition states on the potential energy surface. Zero point energies and thermal en-



ergies at 298.15 K were computed at this level of theory with vibrational frequencies scaled by a factor of 0.95 [25]. A further single point calculation was performed at QCISD(T)/6-31G\*\* level of theory in order to improve the accuracy of the values and to be able to compare the results with previous works [4,26].

### 3. Results and discussion

In agreement with the known unimolecular processes, two pathways are a priori possible for the catalyzed isomerization (Scheme 2). In pathway **a**, the catalyst **M** interacts with one hydrogen of the aldehyde methyl group to yield a complex, which converts into  $[\text{CH}_2\text{CHOH}^+ \dots \text{M}]$  by a 1,3-H transfer and then dissociates. In pathway **b**, **M** interacts in the first step with the hydrogen of the CHO group to give a complex, which converts to  $[\text{CH}_2\text{CHOH}^+ \dots \text{M}]$  by two successive 1,2-H transfers.

In the first part of this work, experimental evidence for the catalyzed tautomerization will be presented, along with the methodology used to choose a catalyst. In a second part, the mechanism of the isomerization will be studied in detail, both by theoretical calculations and experimental studies.

#### 3.1. Experimental evidence for the tautomerization $1 \rightarrow 2$

##### 3.1.1. Methodology: choice of the catalyst and characterization of the ions

In order to find an appropriate catalyst for the isomerization  $1 \rightarrow 2$ , the same reasoning as proposed for catalyzed 1,2-H transfers [6,7] has been used. On one hand, the catalyst **M** must be basic enough to

abstract a proton from ion **1** to give a complex having a structure  $[\text{MH}^+, \text{C}_2\text{H}_3\text{O}^-]$ . This means that, to a first approximation, the proton affinity (PA) of the catalyst must lie above the PA at the carbon site either of the  $\cdot\text{CH}_2\text{CHO}$  radical for pathway **a** or of the carbonyl carbon of the  $\text{CH}_3\text{CO}\cdot$  radical for pathway **b**. On the other hand, M must not be too basic, in order to be able to transfer this proton back to oxygen. This means that its PA must be less than the PA of the  $\cdot\text{CH}_2\text{CHO}$  radical at oxygen. These PA constraints are summarized by

$$\begin{aligned} \text{PA}_{\text{C}}[\cdot\text{CH}_2\text{CHO}] &= \Delta H_f[\text{H}^+] + \Delta H_f[\cdot\text{CH}_2\text{CHO}] \\ &\quad - \Delta H_f[\text{CH}_3\text{CHO}^{\cdot+}] \\ &= 169.4 \pm 2 \text{ kcal mol}^{-1} \end{aligned} \quad (2)$$

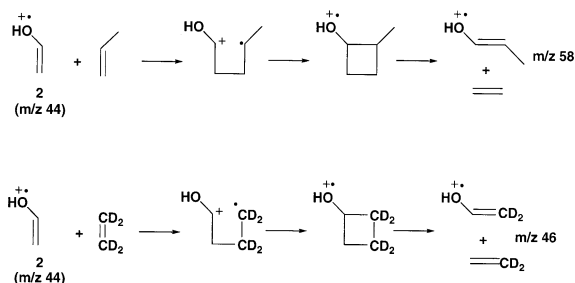
$$\begin{aligned} \text{PA}_{\text{O}}[\cdot\text{CH}_2\text{CHO}] &= \Delta H_f[\text{H}^+] + \Delta H_f[\cdot\text{CH}_2\text{CHO}] \\ &\quad - \Delta H_f[\text{CH}_2\text{CHOH}^{\cdot+}] \\ &= 184.7 \pm 2 \text{ kcal mol}^{-1} \end{aligned} \quad (3)$$

$$\begin{aligned} \text{PA}_{\text{C}}[\text{CH}_3\text{CO}\cdot] &= \Delta H_f[\text{H}^+] + \Delta H_f[\text{CH}_3\text{CO}\cdot] \\ &\quad - \Delta H_f[\text{CH}_3\text{CHO}^{\cdot+}] \\ &= 163.4 \pm 2 \text{ kcal mol}^{-1} \end{aligned} \quad (4)$$

PA's were evaluated from reference data tables [2]. Taking  $\Delta H_f[\cdot\text{CH}_2\text{CHO}] = 0 \text{ kcal mol}^{-1}$  [27] and using Eqs. (2)–(4), we deduced that  $\text{PA}[\text{M}]$  must lie between 169.4 and 184.7  $\text{kcal mol}^{-1}$  when a hydrogen of the methyl group is abstracted in the first step (1,3-H transfer) and between 163.4 and 184.7  $\text{kcal mol}^{-1}$  when the hydrogen of the CHO group is abstracted (double 1,2-H transfer).

Several possible catalysts fulfilling this condition were chosen for the present study, including water ( $\text{PA} = 165.2 \text{ kcal mol}^{-1}$ ) [28], formaldehyde ( $\text{PA} = 170.4 \text{ kcal mol}^{-1}$ ) and methanol ( $\text{PA} = 180.5 \text{ kcal mol}^{-1}$ ). Methanol was also used for more detailed experimental and theoretical mechanistic studies.

In order to characterize the isomerization process, it was necessary to find specific reactions of ions **1** and **2** allowing their identification. Eqs. (2)–(4) indicate that all of the hydrogens of  $\text{CH}_3\text{CHO}^{\cdot+}$  are much



Scheme 3.

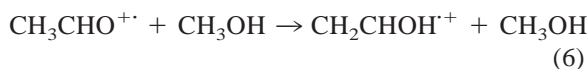
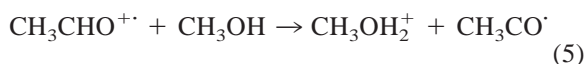
more acidic than the hydroxylic hydrogen of ion **2**, which is, in turn, the most acidic hydrogen in structure **2**. It follows that ions **1** and **2** could then be distinguished by their acidities. Eqs. (2)–(4) also show, in ion **1**, that the hydrogen of the CHO group is more acidic than those of the methyl group. This conclusion was verified experimentally. On one hand, protonation of the neutral partner is very often the dominant reaction of ion **1**, and labeling shows that proton transfer (when it occurs) involves only the hydrogen of the CHO group with the bases used in this study. On the other hand, proton transfer from ion **2** involves the hydroxylic hydrogen [27] and requires neutral partners of higher PA than those used here.

Distinction between **1** and **2** can also be effected by using specific reactions. It is known that  $\text{CH}_2\text{CHOH}^{\cdot+}$  reacts with ethylene or propene by a cycloaddition–cycloreversion process [29]. With propene, the product ion  $\text{CH}_3\text{CHCHOH}^{\cdot+}$  ( $m/z$  58) is formed (Scheme 3). It was verified that  $\text{CH}_3\text{CHO}^{\cdot+}$  does not react in this way but rather by  $\text{H}^\cdot$  abstraction,  $\text{H}^\cdot$  transfer, or charge exchange. Similarly, ion **1** reacts with  $\text{C}_2\text{D}_4$  by  $\text{H}^\cdot$  transfer (efficiency 0.6) to give  $\text{CH}_3\text{CO}^+$  ( $m/z$  43). The enol isomer **2** reacts more slowly (efficiency 0.1) to produce  $\text{CD}_2\text{CHOH}^{\cdot+}$  ( $m/z$  46) through a cycloaddition/cycloreversion reaction (Scheme 3).

### 3.1.2. Experimental proof of the catalyzed isomerization

The reaction of acetaldehyde radical cation **1** with methanol ( $\text{PA} = 180.5 \text{ kcal mol}^{-1}$  [28]) provides the first evidence for the catalyzed isomerization. As expected [Eq. (4)], the reactant ion rapidly disappears at the beginning of the reaction since **1** reacts with

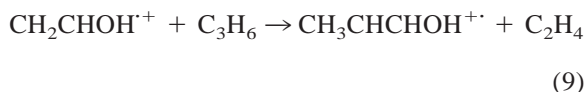
methanol at nearly the collision rate to give an abundant  $m/z$  33 product [proton transfer to methanol, Eq. (5)], and a minor  $m/z$  45 ion (5%, H abstraction from methanol). After some seconds of reaction, the rate of disappearance becomes very low. This result leads to the conclusion that the acetaldehyde radical cation **1** partially isomerizes during the reaction time into a new species. The enol  $\text{CH}_2\text{CHOH}^+$  **2** is a good candidate for this new structure [Eq. (6)], since **2** is the only isomer more stable than **1**, and since it is known to exhibit a lower acidity



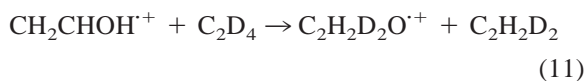
Identification of the isomerized product as the enol isomer **2** was demonstrated by the following experiments.

In the first experiment,  $\text{CH}_3\text{CHO}^{+\cdot}$  **1** generated in the external ion source is trapped in the cell and then allowed to react with a pulse of propene. In this case, apart from  $\text{CH}_3\text{CO}^+$  [ $m/z$  43, H<sup>+</sup> transfer to propene, Eq. (7)] and  $\text{CH}_3\text{CHOH}^+$  [ $m/z$  45, H<sup>+</sup> abstraction from propene, Eq. (8)], the other product ions observed contain only carbon and hydrogen and have been shown to correspond to the self-CI (chemical ionization) spectrum of propene. In the second experiment,  $\text{CH}_2\text{CHOH}^+$  **2** generated in the ion source is thermalized in the cell and is allowed to react with a pulse of propene. The self-CI spectrum of propene is always observed, although to a lesser extent, but the major product ion appears at  $m/z$  58, and was shown by a high resolution mass measurement to be  $\text{C}_3\text{H}_6\text{O}^{+\cdot}$ . This product corresponds to  $\text{CH}_3\text{CHCHOH}^+$  formed by the known cycloaddition–cycloreversion reaction of the ionized enol **2** with propene [29] [Eq. (9), Scheme 3]. In the third experiment,  $\text{CH}_3\text{CHO}^{+\cdot}$  ( $m/z$  44) is allowed to interact in the cell with methanol (pressure =  $1.7 \times 10^{-8}$  mbar,  $t = 2$  s). The main reaction observed is proton transfer. The remaining  $m/z$  44 ions are reisolated prior to admitting a pulse of propene. In this case the product ion  $m/z$  58,  $\text{C}_3\text{H}_6\text{O}^{+\cdot}$ , is also observed (Fig. 2), in a proportion which increases with the initial reaction time with methanol.

This result strongly supports the catalyzed isomerization of  $\text{CH}_3\text{CHO}^{+\cdot}$  into  $\text{CH}_2\text{CHOH}^+$



However, little can be said quantitatively about the extent of isomerization, because of the ions arising from the reaction of propene with ionized propene formed by charge exchange. In an attempt to get more quantitative information about the tautomerization process, several additional experiments were performed. First, ions **1** were isolated in the FTICR cell in the presence of a constant pressure of  $\text{C}_2\text{D}_4$  ( $3 \times 10^{-8}$  mbar), then subjected to a pulse of methanol (peak pressure  $3 \times 10^{-8}$  mbar), and the  $m/z$  44 ions isolated again after 1 s reaction. Further reaction of these ions with  $\text{C}_2\text{D}_4$  (10 s) gives  $\text{CH}_3\text{CO}^+$  ( $m/z$  43, 92%, Eq. (10)), as does ion **1**, along with  $\text{C}_2\text{H}_2\text{D}_2\text{O}^+$  ( $m/z$  46, 8%) as does ion **2** [Eq. (11), Scheme 3]. These conditions (pressure and reaction time) correspond roughly to the half-reaction time of **2** with  $\text{C}_2\text{D}_4$  and to a nearly complete reaction of **1**. Therefore, after the pulse of methanol, the remaining  $\text{C}_2\text{H}_4\text{O}^+$  ions are a mixture of about 85% of unrearranged keto ions **1** and 15% of enol ions **2**



The efficiency of other catalysts was also studied. It was found that water ( $\text{PA} = 165.2 \text{ kcal mol}^{-1}$ ) [28] is unreactive toward isomerization. However, it is interesting to note that the hydrogen of the CHO group is exchanged rapidly in the presence of  $\text{D}_2\text{O}$ .

In the reaction between ion **1** and formaldehyde, the H<sup>+</sup> transfer to  $\text{CH}_2\text{O}$  yields a  $m/z$  43 product and occurs with a fast rate constant ( $k = 10^{-9} \text{ cm}^3 \text{ mol}^{-1} \text{ s}^{-1}$ , efficiency = 0.4). However, after long reaction times (5 s at  $10^{-8}$  mbar), the 10% of the initial  $m/z$  44 ion that remains react very slowly. This

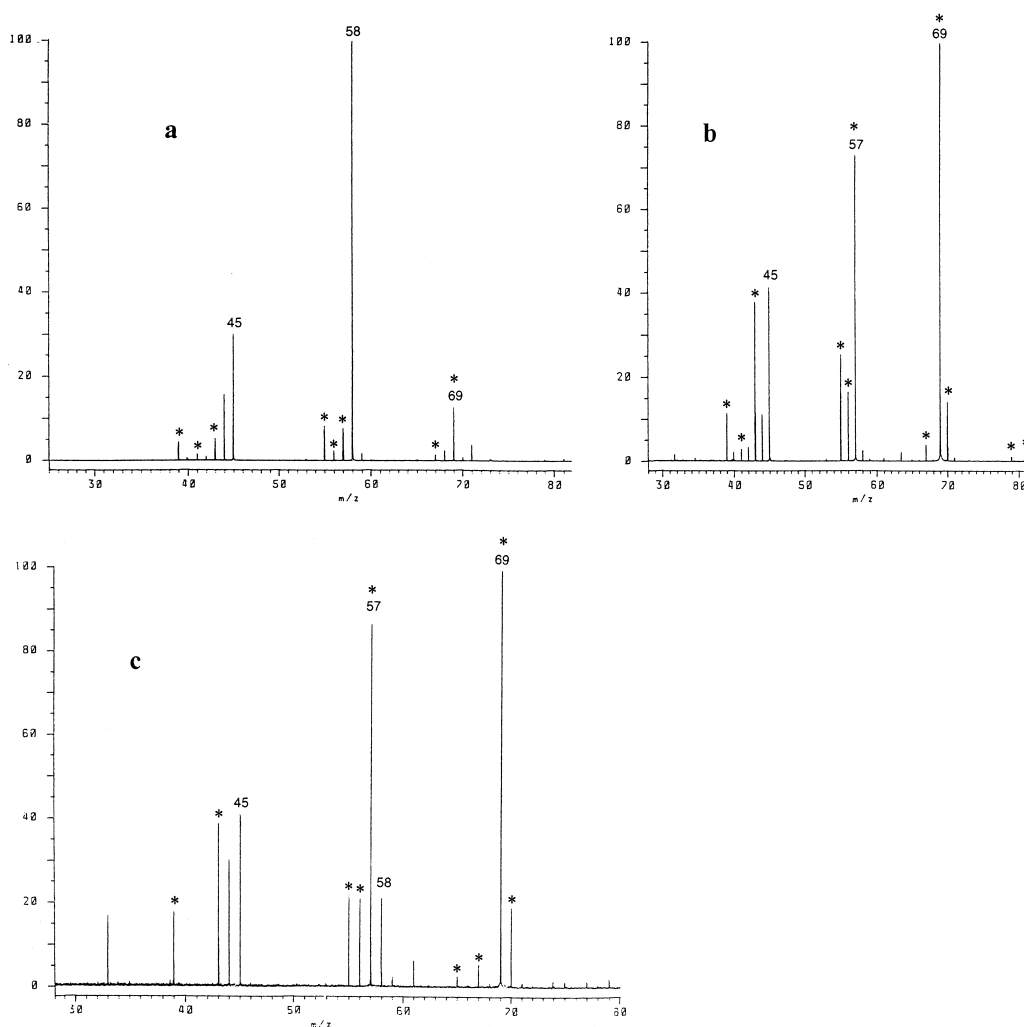


Fig. 2. Reactions of  $m/z$  44 ions with pulsed propene (up to  $10^{-6}$  mbar) (stared peaks arise from the self chemical ionization of propene $^{+}$ ). (a) Pulse of propene on  $\text{CH}_2\text{CHOH}^{+}$ ; (b) pulse of propene on  $\text{CH}_3\text{CHO}^{+}$ ; (c) pulse of propene on  $m/z$  44 ions from  $\text{CH}_3\text{CHO}^{+}$  after 3 s reaction with methanol (pressure  $1.7 \times 10^{-8}$  mbar).

result also suggests the formation of ion **2**, since **2** does not protonate  $\text{CH}_2\text{O}$  but instead reacts only slowly by H $^+$  abstraction to give the  $m/z$  45 product ion ( $m/z$  46 with  $\text{CD}_2\text{O}$ ). Structure **2** was also characterized by using  $\text{C}_2\text{D}_4$  (2 pulses, peak pressure  $10^{-7}$  mbar). A  $\text{C}_2\text{H}_2\text{D}_2\text{O}^{+}$  product ion ( $m/z$  46) was also observed in this case, although in smaller proportion than when methanol is used as the catalyst. Since it seemed to be the best catalyst, calculations and further experiments were performed using methanol.

### 3.2. Mechanism of tautomerization

As outlined in sec. 1, two mechanisms are a priori possible for the keto-enol tautomerization (Scheme 2). The pathway **a** involves a 1,3-H transfer, whereas the pathway **b** requires two successive H transfers. The potential energy surface of the  $[\text{C}_2\text{H}_4\text{O}^{+}, \text{CH}_3\text{OH}]$  system was explored theoretically, and compared with experiments involving D-labeled compounds.



Table 1

Calculated electronic energies (in Hartrees) and relative energies (in kcal mol<sup>-1</sup>) for the different structures

	MP2/ 6-31G**	QCISD(T)/ 6-31G**	$\Delta$ MP2/ 6-31G**	$\Delta E_{298.15}^{\circ}$ $\Delta$ MP2/6-31G**	$\Delta$ QCISD(T)/ 6-31G**	$\Delta E_{298.15}^{\circ}$ QCISD(T)/ 6-31G**
CH <sub>3</sub> OH	-115.382 01	-115.412 44				
CH <sub>3</sub> O <sup>•</sup>	-114.709 90	-114.746 50				
CH <sub>3</sub> CHO <sup>•+</sup> (1)	-153.001 28	-153.057 71				
CH <sub>3</sub> COH <sup>+</sup>	-153.008 66	-153.051 82				
CH <sub>3</sub> CHOH <sup>+</sup>	-153.685 70	-153.730 39				
CH <sub>2</sub> CHOH <sup>+</sup> (2)	-153.035 54	-153.079 12				
CH <sub>3</sub> OH <sub>2</sub> <sup>+</sup>	-115.689 43	-115.722 11				
CH <sub>2</sub> COH <sup>•</sup>	-152.669 95	-152.717 22				
CH <sub>2</sub> CHO <sup>•</sup>	-152.710 06	-152.759 99				
CH <sub>3</sub> CO <sup>•</sup>	-152.734 31	-152.772 93				
<b>1</b> + CH <sub>3</sub> OH	-268.383 29	-268.470 15	0.0	0.0	0.0	0.0
<b>2</b> + CH <sub>3</sub> OH	-268.418 55	-268.491 56	-21.5	-20.0	-13.4	-12.0
CH <sub>3</sub> COH <sup>+</sup> + CH <sub>3</sub> OH	-268.390 67	-268.464 26	-4.6	-3.9	3.7	4.4
CH <sub>3</sub> O <sup>•</sup> + CH <sub>3</sub> CHOH <sup>+</sup>	-268.395 60	-268.476 89	-7.7	-6.8	-4.2	-3.3
CH <sub>3</sub> OH <sub>2</sub> <sup>+</sup> + CH <sub>2</sub> CHO <sup>•</sup>	-268.399 49	-268.482 10	-10.2	-9.0	-7.5	-6.3
CH <sub>3</sub> OH <sub>2</sub> <sup>+</sup> + CH <sub>3</sub> CO <sup>•</sup>	-268.423 74	-268.495 04	-25.4	-23.7	-15.6	-13.9
<b>3</b>	-268.431 03	-268.507 93	-30.0	-24.8	-23.7	-18.6
<b>4</b>	-268.436 53	-268.518 95	-33.4	-31.2	-30.6	-28.4
<b>5a</b>	-268.468 38	-268.541 34	-53.4	-50.3	-44.7	-41.6
<b>5b</b>	-268.471 07	-268.543 79	-55.1	-52.1	-46.2	-43.2
<b>6</b>	-268.456 99	-268.526 98	-46.3	-42.3	-35.7	-31.7
<b>7</b>	-268.466 19	-268.537 35	-52.0	-48.3	-42.2	-38.6
<b>8</b>	-268.442 28	-268.513 76	-37.0	-32.6	-27.4	-23.0
<b>TS 3/6</b>	-268.407 82	-268.495 04	-15.4	-13.8	-15.6	-14.0
<b>TS 4/5a</b>	-268.397 02	-268.478 46	-8.6	-9.7	-5.2	-6.3
<b>TS 6/7</b>	-268.454 46	-268.524 97	-44.7	-41.4	-34.4	-31.1
<b>TS 7/8</b>	-268.424 09	-268.497 58	-25.6	-22.6	-17.2	-14.2
<b>TS 8/5b</b>	-268.390 61	-268.469 47	-4.6	-3.7	-0.4	1.4
<b>TS 7/5b</b>	-268.389 96	-268.463 32	-4.2	-4.3	4.3	4.2
<b>TS 5a/5b</b>	-268.448 60	-268.525 23	-41.0	-37.3	-34.6	-30.9

### 3.2.1. Calculation of energy profiles

The potential energy profiles of the two reaction pathways **a** and **b** shown in Scheme 2 were calculated for M = methanol. The enthalpies of the stable minima as well as of the saddle points are reported in Table 1 and the geometries of the corresponding structures are shown in Figs. 3 and 4.

The potential energy profile of pathway **a**, involving a 1,3-H transfer, is shown in Fig. 5. In this pathway the first step is the approach of the methanol to the side of acetaldehyde opposite to the hydrogen of the CHO group. This yields a stable intermediate complex **3**, in which methanol interacts both with a hydrogen of the methyl group and with the positively charged oxygen of the acetaldehyde radical cation.

Structure **3** undergoes interconversion with the more stable ion **4**. Ions **3** and **4** each exhibit a strong interaction energy (18.6 and 28.4 kcal mol<sup>-1</sup>, respectively) between the acetaldehyde and methanol moieties, which leads to significant internal energies in these complexes. They therefore possess sufficient internal energy to overcome subsequent intermediate energy barriers.

The structure of **3** is rather surprising. Since the PA of methanol (180.5 kcal mol<sup>-1</sup> [28]) lies some 10 kcal mol<sup>-1</sup> above that of the <sup>•</sup>CH<sub>2</sub>CHO radical [Eq. (2)], a structure involving protonated methanol bonded to the <sup>•</sup>CH<sub>2</sub>CHO radical might have been expected. But the two center–three electron interaction between the oxygens, as indicated by the short (2.11 Å) O–O

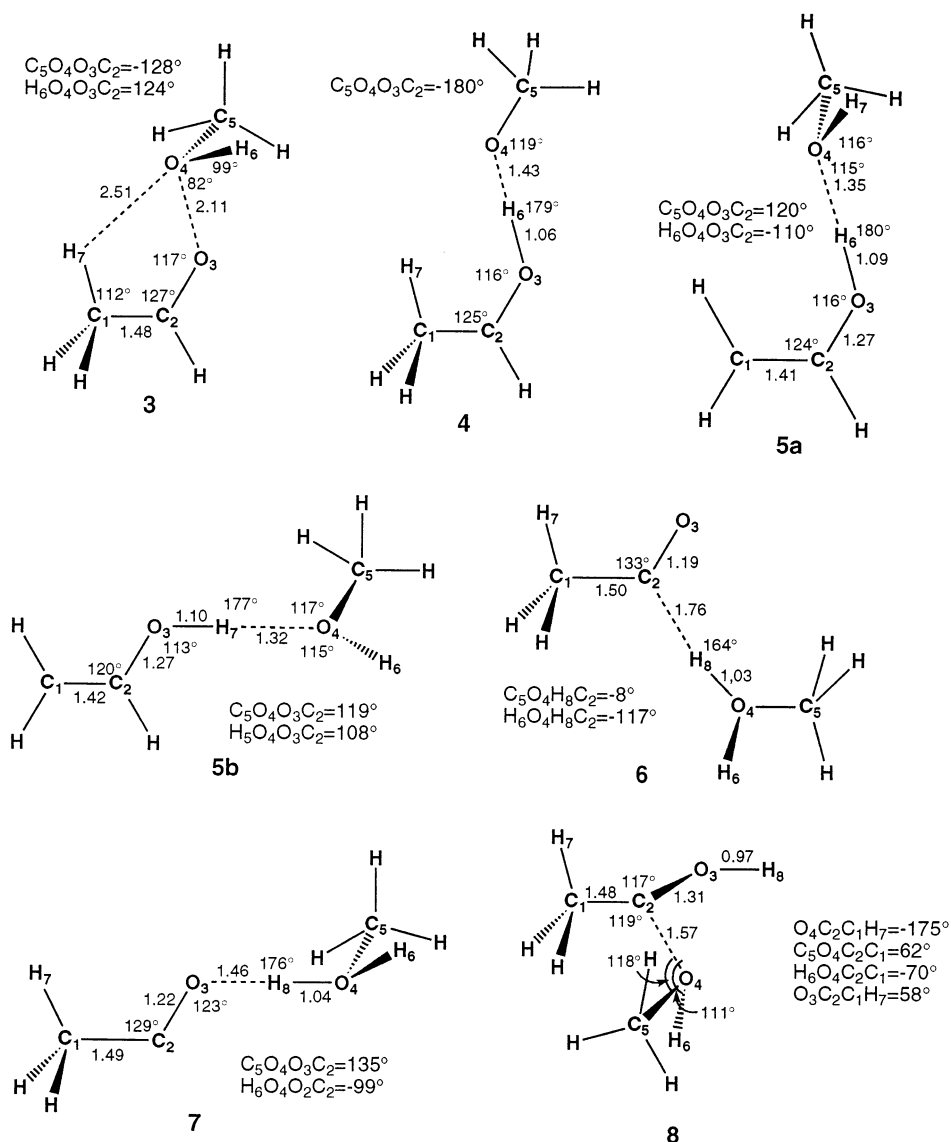


Fig. 3. UMP2/6-31G\*\* optimized structures of the stable states.

distance, provides the system with a more energetically favorable structure. For this reason, the oxygen of methanol abstracts a proton less easily than expected, which accounts for the weak interaction of methanol with the hydrogen of the methyl group of **1**. Thus, starting from structure **3**, H transfer is preceded by a conversion of **3** into **4** through  $TS_{3/4}$ . Unfortunately,  $TS_{3/4}$  is the only transition state which has not been located. Other authors [26] have encountered the

same difficulty in locating a similar transition state and have considered that the barrier should not be very large. The formation of complex **4** from **3** is however strongly supported by the product ion at  $m/z$  45 (5%, see above), which was experimentally shown to involve the selective abstraction of the hydroxylic hydrogen of methanol [30].

The intermediate **4** resembles protonated aldehyde bonded to a methoxy radical. In this complex, the



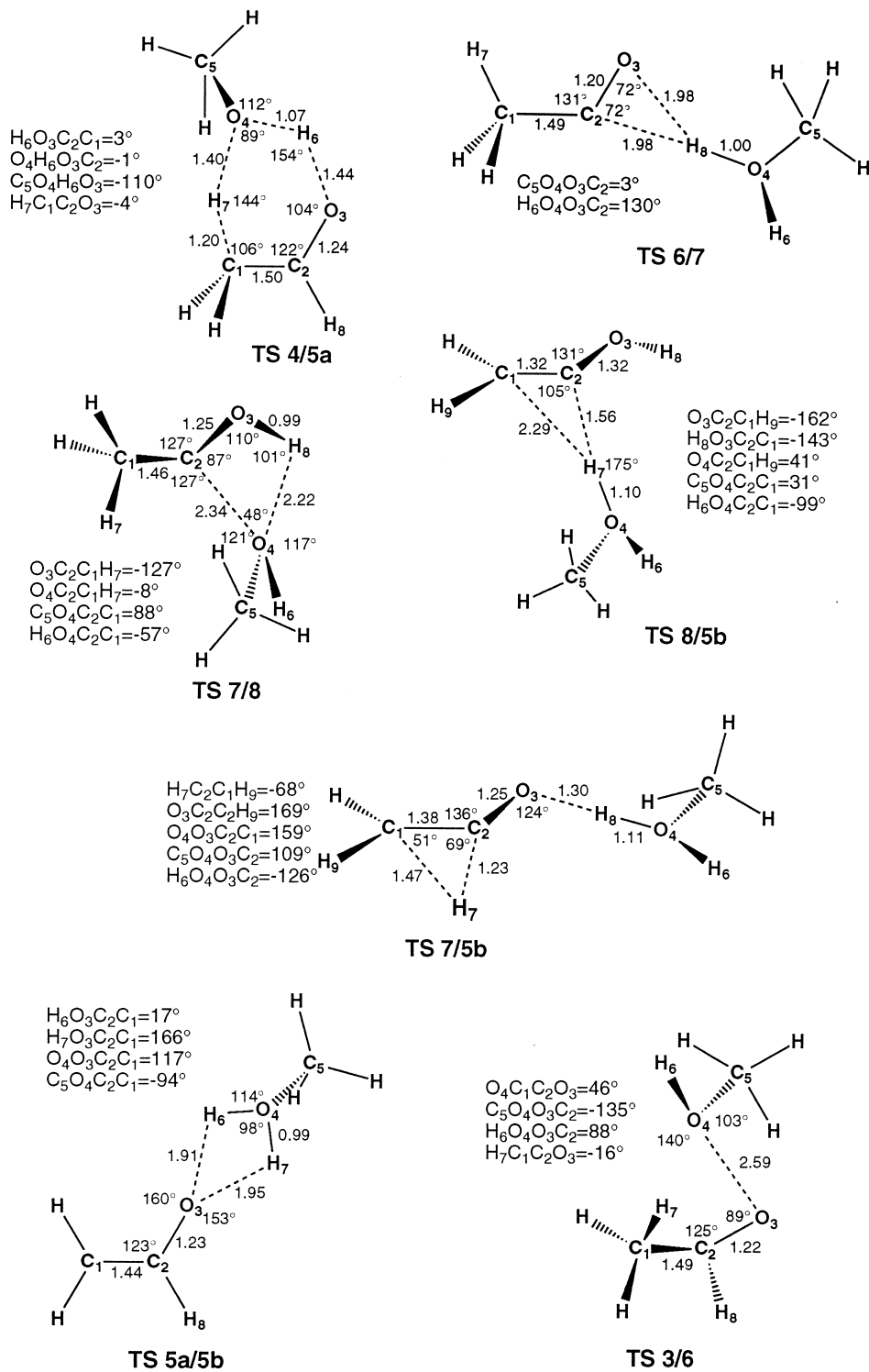


Fig. 4. UMP2/6-31G\*\* optimized structures of the transition states.

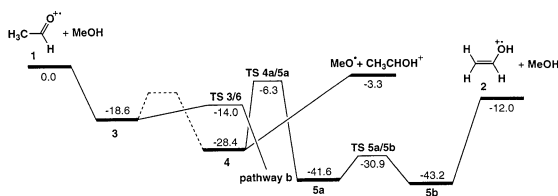


Fig. 5. Potential energy profile for pathway **a** (kcal mol<sup>-1</sup>).

neutral methoxy abstracts a methyl hydrogen from the aldehyde moiety, which converts **4** into **5** through a six membered transition state **TS**<sub>4/5a</sub>. The complex **5a**, which corresponds to an enol radical cation H bonded to a molecule of methanol, is strongly stabilized (41.6 kcal mol<sup>-1</sup>) with respect to the reactant energy. A rotation of the methanol moiety allows **5a** to convert into **5b**. These species differ only by the syn/anti conformation of the hydrogen. Interconversion between **5a** and **5b** via **TS**<sub>5a/5b</sub> (-30.9 kcal mol<sup>-1</sup>) leads to the permutation of the hydroxylic hydrogen of methanol and one of the hydrogens initially borne by the methyl group of acetaldehyde. Dissociation of either rotamer of **5** leads to the final products (CH<sub>2</sub>CHOH<sup>+</sup> + CH<sub>3</sub>OH), located 12.0 kcal mol<sup>-1</sup> below the energy of the reactants. The other possible cleavage, giving protonated methanol and the <sup>•</sup>CH<sub>2</sub>CHO radical, is an energetically less favourable outcome (-6.3 kcal mol<sup>-1</sup>, Table 1).

The transition state **TS**<sub>4/5a</sub> is a six membered ring with two hydrogen atoms interacting with MeO<sup>•</sup> on one side and <sup>•</sup>CH<sub>2</sub>CHO on the other side [31]. **TS**<sub>4/5a</sub> lies only 6.3 kcal mol<sup>-1</sup> below the reactants in energy. We conclude that **TS**<sub>4/5a</sub> represents the rate determining barrier.

Starting from intermediates **3** and **4**, two processes can take place. Intermediate **4** can isomerize into the complex **5a**. A second pathway involves the isomerization of **3** leading to **6** (see pathway **b**) via **TS**<sub>3/6</sub> (-14.0 kcal mol<sup>-1</sup>), which is a possible outcome. This competition is reflected in two experimental results. First, the isomerization is slow (less than 5% of the overall process). Second, as outlined below, a dramatic isotope effect is observed when CD<sub>3</sub>CHO<sup>+</sup> is used as the reactant ion. It may be noted that no pathway connecting **3** directly to **5a/b** was found at the UMP2/6-31G\*\* level used in this work.

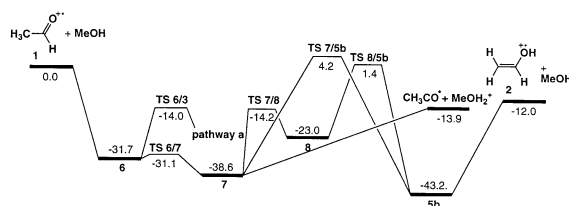


Fig. 6. Potential energy profile for pathway **b** (kcal mol<sup>-1</sup>).

The pathway **b** involving a catalyzed double 1,2-H transfer begins with the interaction of methanol with the hydrogen of the CHO group of ion **1**. A barrier-free proton transfer leads directly to the low-lying complex **6**, which possesses a substantial internal energy (31.7 kcal mol<sup>-1</sup>). The complex **6** may be considered as protonated methanol electrostatically bonded to a CH<sub>3</sub>CO<sup>•</sup> radical. It interconverts with complex **7**, which is, in fact, protonated methanol H bonded with the same radical but in this case at the oxygen. The isomerization **6** → **7** via **TS**<sub>6/7</sub> is very facile, since this region of the potential energy surface (PES) is almost flat. Therefore this step, corresponding to the first 1,2-H transfer, cannot be rate determining in the overall isomerization process (Fig. 6).

In contrast, Fig. 6 shows that **7** → **5b**, corresponding to the second 1,2-H transfer, is the rate determining step. Two possible pathways were found for this conversion. Ion **7** is almost linear, and its conversion to **5b** can occur by a direct 1,2-H shift analogous to that observed in the isolated ion [4]. As expected, the corresponding barrier is high and **TS**<sub>7/5b</sub> lies +4.2 kcal mol<sup>-1</sup> above the energy of the isolated reactants. A second possible path corresponds to a catalyzed 1,2-H transfer. On this pathway a stable state **8** was found, linked to ion **7** by turning the methanol molecule with respect to the ion. The transition state **TS**<sub>7/8</sub> was found 14.2 kcal mol<sup>-1</sup> below the reactants' energy. The methanol molecule can then catalyze proton transfer to yield the complex **5b** through a three-membered transition state **TS**<sub>8/5b</sub> located at +1.4 kcal mol<sup>-1</sup> relative to the reactants' energy.

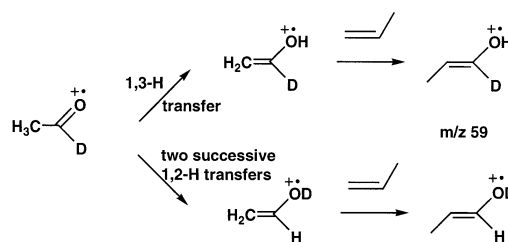
It is essential to point out that the most favourable outcome for the reaction of complexes **6** and **7** (in terms of both energy barriers and overall enthalpy) is the simple cleavage leading to protonated methanol.

For the two pathways **a** and **b** described above, the last question to be answered is whether they are independent? The two pathways can only cross between structures **3** and **6**. The transition state  $\text{TS}_{3/6}$  is found to be  $14.0 \text{ kcal mol}^{-1}$  below the reactants' energy, which means that the simple cleavage of **6** ( $-13.9 \text{ kcal mol}^{-1}$ ) is significantly more favoured than the conversion  $\mathbf{6} \rightarrow \mathbf{3}$  for entropic reasons. It is therefore very unlikely that pathway **b** would interfere in what is occurring in pathway **a**. The reverse is however not true, because the conversion  $\mathbf{3} \rightarrow \mathbf{6}$  is one of the energetically allowed channels in pathway **a**.

In conclusion, the ab initio calculations results can be summarized in the following statements. (1) Only pathways **a** can lead to isomerization  $\mathbf{1} \rightarrow \mathbf{2}$  via a six-membered transition state in which the hydroxylic hydrogen of methanol must be completely, (or partially, if  $\mathbf{5a} \leftrightarrow \mathbf{5b}$  takes place), incorporated in the final enol ion. (2) Pathway **b** leads easily to the protonation of methanol, which is therefore an open channel for this mechanism. (3) Ions **6** and **7** of pathway **b** do not isomerize into ions **3** and **4** of pathway **a**.

### 3.2.2. Isomerization mechanism: experimental study

The different steps of the mechanism suggested by the calculations may now be discussed in the light of the experimental results. From the preceding experimental results, it would appear facile to distinguish between pathways **a** and **b** by using labeled ions **1**. In fact, this is difficult for at least four reasons. (1) The isomerization process is, in all cases, in competition with proton transfer reactions, which reduces the yield of ions **2**. (2) It is not easy to distinguish pathways **a** and **b** by the position of the deuterium atoms in the isomerized ions **2**. Indeed, the two pathways for isomerization of  $\text{CH}_3\text{CDO}^+$  lead, respectively, to  $\text{CH}_2\text{CDOH}^+$  and  $\text{CH}_2\text{CHOD}^+$   $m/z$  45 ions, which yield two isobaric  $m/z$  59 ions when they undergo a cycloaddition/cycloreversion reaction with propene (Scheme 4). (3)  $\text{CH}_3\text{CHO}^+$  exchanges the hydrogen of the CHO group in the presence of  $\text{D}_2\text{O}$ , which prevents the use of this reactant to characterize the hydroxylic hydrogen of ion **2** by H/D exchange. (4)



Scheme 4.

Each of these isomerizations exhibits a strong isotope effect whose interpretation is not unambiguous. For instance, no significant isomerization of  $\text{CD}_3\text{CHO}^+$  by methanol could be significantly detected by pulsing in propene under the same conditions as those described for unlabeled acetaldehyde. Although the low extent of isomerization in these experiments [see Fig. 2(c)] does not allow a quantitative evaluation of this isotope effect, it should be undeniably large. This could be indicative of an isotope effect in pathway **a** as well as in the second H-transfer in pathway **b**. Indeed, calculations show that both transfers are rate determining.

However, the reaction of  $\text{CH}_3\text{CDO}^+$  ( $m/z$  45) with  $\text{CH}_3\text{OH}$  (pressure  $10^{-8}$  mbar) provides insight into the isomerization mechanism. After 4 s of reaction, a pulse of propene on the reisolated remaining  $m/z$  45 ions gives  $\text{C}_3\text{H}_5\text{DO}^+$  product ions ( $m/z$  59), as expected from a cycloaddition/cycloreversion with the monodeuterated enol ion **2**. Once again, the yield of  $m/z$  59 ions increases with initial reaction time, in agreement with a greater proportion of remaining  $m/z$  45 ions being isomerized to the enol structure. Further reaction with  $\text{CH}_3\text{OH}$  does not lead to any significant yield of  $\text{C}_3\text{H}_6\text{O}^+$  ions ( $m/z$  58), even after 10 s reaction time, demonstrating that these  $\text{C}_3\text{H}_5\text{DO}^+$  ions do not exchange deuterium with methanol. This indicates that the deuterium atom has remained attached to the original carbon atom in the isomerization process  $\mathbf{1} \rightarrow \mathbf{2}$ , and that, in this case, pathway **a** is operative. Actually, under the same conditions, the selectively prepared enol ion  $\text{CH}_3\text{CHCHOH}^+$  exchanges its hydroxyl hydrogen with  $\text{CH}_3\text{OD}$  (pressure  $10^{-8}$  mbar, half reaction time 10 s).

In the isomerization experiment using  $\text{CH}_3\text{CDO}^+$

as reactant ion, pathway **b** does not operate, since it would lead to a  $\text{CH}_2\text{CHOD}^+$  product, which is not observed. However, this result cannot be considered as a definitive proof that pathway **b** is not operative in the blank experiment, because it could be a priori interpreted by a strong isotope effect inhibiting the 1,2-D transfer in the reaction  $\mathbf{6} \rightarrow \mathbf{7}$ . However, considering that calculations demonstrate that this step is not rate determining pathway **b**, it can be concluded that the double 1,2-H transfer does not take place.

Does the catalyzed 1,3-H transfer occurs via the six-membered transition state  $\text{TS}_{4/5a}$ ? In order to answer this question, the reaction of the acetaldehyde radical cation with  $\text{CH}_3\text{OD}$  was performed in the cell. In order to avoid any H/D exchange between the hydrogen of the CHO group and the deuterium atom of  $\text{CH}_3\text{OD}$ ,  $\text{CH}_3\text{CDO}^+$  ( $m/z$  45) was chosen as the reactant ion. After 6 s of reaction (pressure =  $10^{-8}$  mbar), the  $m/z$  45 ( $\text{C}_2\text{H}_3\text{DO}^+$ ) and  $m/z$  46 ( $\text{C}_2\text{H}_2\text{D}_2\text{O}^+$ ) products were selected. These products react with pulsed propene by cycloaddition/cycloreversion to yield the  $m/z$  59 ( $\text{C}_3\text{H}_5\text{DO}^+$ ) and  $m/z$  60 ( $\text{C}_3\text{H}_4\text{D}_2\text{O}^+$ ) enol ions in almost equal abundance. The  $m/z$  59 enol then exchanges its hydroxylic hydrogen slowly with  $\text{CH}_3\text{OD}$ .

This result proves that there is an intermediate complex in the pathway **a** possessing a structure in which there is a  $\text{CH}_3\text{OH}_2^+$  moiety which allows a symmetrisation of the position of one methyl hydrogen of the ion and the hydroxylic hydrogen of methanol. The structures drawn Fig. 5 indicate that this intermediate cannot be **3** nor **4**. In contrast, **5a** is a good candidate, because its interconversion with **5b** prior to dissociation leads to a  $\text{CH}_2\text{CHOH}^+$  final product whose enolic hydrogen is (in agreement with the preceding experiment) either the hydroxylic hydrogen of methanol (50%) or a methyl hydrogen of the reactant acetaldehyde.

Finally, calculations suggest that ion **6** in pathway **b** does not isomerize into ion **3** in pathway **a**. An experimental demonstration can be given. In pathway **b**, the structures of ions **6** and **7** contain a protonated methanol moiety, leading to a symmetrization of the hydrogen of CHO and the hydroxylic hydrogen of

methanol. Should this isomerization precede the pathway **a**, the previous paragraph shows that the hydrogen of the CHO group must be partially expelled at the end of the isomerization process. This partial elimination was not observed in any experiment using labeled ions or labeled reactants.

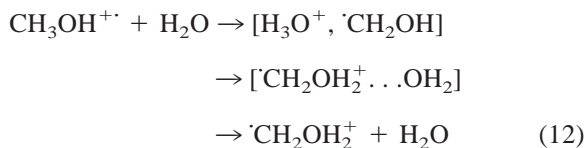
### 3.2.3. Comparison with the isomerization of isolated ions

Comparison of the energy profiles for the solvated ion **1** (Figs. 5 and 6) and that calculated by Bertrand and Bouchoux for the isolated ions [4] (Fig. 1) leads to conclusions which are only suggestive (since the calculational methods are different), but which are nevertheless very interesting.

For 1,3-H transfer in isolated ions **1** and **2**, isomerizing  $\text{CH}_3\text{CHO}^+$  to  $\text{CH}_2\text{CHOH}^+$ , the energy barrier is greater than  $38 \text{ kcal mol}^{-1}$ . The corresponding barrier is only  $12.3 \text{ kcal mol}^{-1}$  for the solvated ions (Fig. 5), showing a moderate but real catalytic effect of methanol.

A more pronounced contrast appears when the processes involving a double 1,2-H transfer are compared. For the isolated ions (Fig. 1), both steps involve substantial barriers, while only one pathway is observed for solvated ions. The isomerization  $\text{CH}_3\text{CHO}^+ \rightarrow \text{CH}_2\text{COH}^+$  requires  $37.3 \text{ kcal mol}^{-1}$  in the unimolecular process but only  $0.6 \text{ kcal mol}^{-1}$  in the catalyzed process ( $\mathbf{6} \rightarrow \mathbf{7}$ ). In contrast, the barriers are comparable for  $\text{CH}_2\text{CHOH}^+ \rightarrow \text{CH}_3\text{COH}^+$  and  $\mathbf{5b} \rightarrow \mathbf{7}$ , since the transition state lies  $43.5 \text{ kcal mol}^{-1}$  above the final state in the first case and  $44.6 \text{ kcal mol}^{-1}$  in the second.

The mechanism of the reaction  $\mathbf{6} \rightarrow \mathbf{7}$  is very similar to that of the catalyzed 1,2-H transfer involved in the isomerization of ionized methanol to its distonic counterpart [6,7]. In this case, interaction between the ion and the neutral gives the complex  $[\text{H}_3\text{O}^+, \text{CH}_2\text{OH}]$  whose conversion into  $[\text{CH}_2\text{OH}_2^+ \dots \text{OH}_2]$  requires an energy barrier of only  $2 \text{ kcal mol}^{-1}$



Therefore, the question remains of understanding why the catalyst is not efficient in the 1,2-H transfer  $7 \rightarrow 5b$ . Our interpretation, given below, again underlines the role of the PA of the catalyst in determining its efficiency.

### 3.2.4. Role of the PA of the catalyst

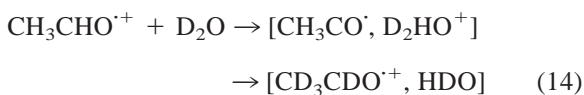
Catalysis is not efficient for the  $8 \rightarrow 5$  transfer step because methanol is not basic enough to abstract a proton from the  $\text{CH}_3\text{COH}^+$  ionized carbene. It can first be observed that in the complex **8**, the primary hydrogen to be transferred is clearly on the carbon of the ion and far from the oxygen of methanol. Second, the PA of the radical can be evaluated from

$$\begin{aligned} \text{PA}_C[\text{CH}_2=\dot{\text{C}}\text{OH}] &= \Delta H_f[\text{H}^+] + \Delta H_f[\text{CH}_2=\dot{\text{C}}\text{OH}] \\ &\quad - \Delta H_f[\text{CH}_3\dot{\text{C}}^+\text{OH}] \\ &= 187.3 \pm 2 \text{ kcal/mol}^{-1} \quad (13) \end{aligned}$$

By using  $\Delta H_f[\text{CH}_3\text{COH}^+] = 199.4 \text{ kcal mol}^{-1}$  [32] and  $\Delta H_f[\text{CH}_2\text{COH}] = 21 \text{ kcal mol}^{-1}$  [33],  $187.3 \text{ kcal mol}^{-1}$  is found for  $\text{PA}_C[\text{CH}_2\text{COH}]$ , which is significantly higher than  $\text{PA}[\text{methanol}]$  ( $180.5 \text{ kcal mol}^{-1}$ ) [28].

It should be outlined that it is not possible to find another molecule which could operate in the isomerization  $7 \rightarrow 5$ , since the PA of the catalyst must lie above  $187.3 \text{ kcal mol}^{-1}$  in order to abstract the proton from the methyl group [Eq. (14)]. At the same time, it must be less than  $184.7 \text{ kcal mol}^{-1}$  in order to give the proton back to the oxygen from the methyl group [Eq. (3)].

Reaction of ion **1** with  $\text{D}_2\text{O}$  also illustrates the importance of the PA of the catalyst. The PA of water ( $165.2 \text{ kcal/mol}$ ) is not great enough to permit pathway **a** by abstraction of a primary hydrogen of ion **1** [Eq. (2)]. In contrast, the PA of water allows the first 1,2-H transfer of pathway **b** [Eq. (4)], but not the second. As a consequence, it was experimentally found that in the presence of  $\text{D}_2\text{O}$ , ion **1** exchanges the hydrogen of the CHO group rapidly by the mechanism depicted schematically in



## 4. Conclusion

FTICR experiments show that different molecules catalyze the hydrogen transfer converting ionized acetaldehyde **1** into its ionized vinyl alcohol counterpart **2**, which has been characterized by its specific behaviour toward selected reactants. This catalyzed isomerization occurs by a direct 1,3-H transfer (pathway **a**) and not by two successive 1,2-H transfers (pathway **b**). Using methanol as catalyst, the different steps of the process were elucidated using both calculations and experiments with labeled reactants. Pathway **a** begins with the formation of a highly stabilized complex **3**, involving a two center–three electron interaction between the two oxygen atoms and an interaction between a hydrogen of the methyl group of **1** and the oxygen of methanol. This complex isomerizes into a complex **4**, which in turn isomerizes, via a six membered transition state, to **5a** (corresponding to ionized vinylalcohol H bonded to the oxygen of methanol), which dissociates to yield ion **2**. The catalysis is better described as a hydrogen atom transport than by a proton transport.

Pathway **b** begins with the interaction between the hydrogen of the CHO group and the oxygen of methanol to give complex **6** and then **7**, both of which correspond to protonated methanol H bonded to a  $\text{CH}_3\text{CO}^+$  radical. Dissociation of **7** to give protonated methanol is strongly favoured relative to the isomerization leading to ionized vinyl alcohol.

Compared to the unimolecular behaviour of bare ions **1** and **2** (which are connected either by a direct 1,3-H transfer or by a double 1,2-H transfer), the reaction of **1** with methanol catalyzes the first pathway, while the second one is inhibited.

This knowledge of the catalyzed isomerization of ions is equally important for the understanding of bimolecular ion–molecule reactions as for reaction within complexes formed by cleavage of a radical cation.

## References

- [1] J.R. Keeffe, A.J. Kresge, in *The Chemistry of Enols*, Z. Rappoport (Ed.), Wiley, Chichester, UK, 1990, p. 399.

- [2] S.G. Lias, J.E. Bartmess, J.F. Liebman, J.L. Holmes, R.D. Levin, W.G. Mallard, *J. Phys. Chem. Ref. Data* 1 (1988) 17 (suppl.).
- [3] (a) G. Bouchoux, *Mass Spectrom. Rev.* 7 (1988) 1; (b) F. Turecek, in *The Chemistry of Enols*, Z. Rappoport (Ed.), Wiley, Chichester, UK, 1990, p. 95; (c) Y. Apeloig *ibid.*, p. 48.
- [4] W. Bertrand, G. Bouchoux, *Rapid Commun. Mass Spectrom* 12 (1998) 1697, and references cited therein.
- [5] D.K. Bohme, *Int. J. Mass Spectrom. Ion Processes* 115 (1992) 95.
- [6] H.E. Audier, D. Leblanc, P. Mourgues, T.B. McMahon, S. Hammerum, *J. Chem. Soc., Chem. Commun.* (1994) 2329.
- [7] J.W. Gauld, L. Radom, J. Fossey, H.E. Audier, *J. Am. Chem. Soc.* 118 (1996) 6299.
- [8] H.E. Audier, J. Fossey, P. Mourgues, T.B. McMahon, S. Hammerum, *J. Phys. Chem.* 100 (1996) 18380.
- [9] P.K. Chou, R.L. Smith, L.J. Chyall, H.I. Kenttämä, *J. Am. Chem. Soc.* 117 (1995) 4374.
- [10] S.P. de Visser, L.J. de Koning, N.M.M. Nibbering, *J. Am. Chem. Soc.* 120 (1998) 1517.
- [11] S. Kato, C.H. DePuy, S. Gronert, V.M. Bierbaum, *J. Am. Soc. Mass Spectrom.* 10 (1999) 840, and references cited therein.
- [12] H.E. Audier, T.B. McMahon, *J. Mass Spectrom.* 32 (1997) 201.
- [13] S. Okada, Y. Abe, S. Tanigushi, S. Yamabe, *J. Am. Chem. Soc.* 109 (1987) 296.
- [14] G. van der Rest, P. Mourgues, J. Fossey, H.E. Audier, *Int. J. Mass Spectrom. Ion Processes* 160 (1997) 107.
- [15] J. Chamot-Rooke, G. van der Rest, P. Mourgues, H.E. Audier, *Int. J. Mass Spectrom.* 195 (2000) 385.
- [16] H. Becker, D. Schröder, W. Zummack, H. Schwarz, *J. Am. Chem. Soc.* 116 (1994) 1096.
- [17] G. van der Rest, P. Mourgues, J. Tortajada, H.E. Audier, *Int. J. Mass Spectrom. Ion Processes* 179/180 (1998) 293.
- [18] (a) G. van der Rest, J. Chamot-Rooke, P. Mourgues, D. Leblanc, H.E. Audier, *Proceedings of the 14th International Mass Spectrometry Congress, Tampere, Finland, 1997*, p. 185; (b) G. van der Rest, H.E. Audier, P. Mourgues, *Proceedings des 15èmes Journées Françaises de Spectrométrie de Masse, Lyon, France, 1998*, p. 45.
- [19] M.A. Trikoupi, J.K. Terlouw, *J. Am. Chem. Soc.* 120 (1998) 12131.
- [20] P. Kofel, M. Allemann, H.P. Kellerhals, K.P. Wanczek, *Int. J. Mass Spectrom. Ion Processes* 65 (1985) 97.
- [21] P. Caravatti, M. Allemann, *Org. Mass Spectrom.* 26 (1991) 514.
- [22] T. Su, W.J. Chesnavich, *J. Phys. Chem.* 76 (1982) 9183.
- [23] M.J. Frisch, G.W. Trucks, H.B. Schlegel, P.N.W. Gill, B.G. Johnson, M.A. Robb, J.R. Cheeseman, T.A. Keith, G.A. Petersson, J.A. Montgomery, K. Raghavachari, M.A. Al-Laham, V.G. Zakrzewski, J.V. Ortiz, J.B. Foresman, J. Cioslowski, B.B. Stefanov, A. Nanayakkara, M. Challacombe, C.Y. Peng, P.Y. Ayala, W. Chen, M.W. Wong, J.L. Andres, E.S. Replogle, R. Gomperts, R.L. Martin, D.J. Fox, J.S. Binkley, D.J. DeFrees, J. Baker, J.P. Stewart, M. Head-Gordon, C. Gonzalez, J.A. Pople, GAUSSIAN 94, Revision B.2, Gaussian Inc., Pittsburgh, PA, 1995.
- [24] (a) C. Møller, M.S. Plesset, *Phys. Rev.* 46 (1934) 618; (b) R. Khrisnan, J.A. Pople, *Int. J. Quantum Chem., Symp.* 14 (1980) 91; (c) P.C. Hariharan, J.A. Pople, *Theor. Chim. Acta* 28 (1973) 213; (d) J.A. Pople, A.P. Scott, M.W. Wong, L. Radom, *Isr. J. Chem.* 33 (1993) 345.
- [25] L.A. Curtiss, K. Raghavachari, G.W. Trucks, J.A. Pople, *J. Chem. Phys.* 94 (1991) 7221.
- [26] P.C. Burgers, L.M. Fell, A. Milliet, M. Rempp, P.J. Ruttink, J.K. Terlouw, *Int. J. Mass Spectrom. Ion Processes* 167/168 (1997) 291.
- [27] H.E. Audier, G. Bouchoux, P. Mourgues, F. Berruyer-Penaud, *Org. Mass Spectrom.* 27 (1992) 439.
- [28] E. Hunter, S.G. Lias, *J. Chem. Phys. Ref. Data* 27 (1998) 413.
- [29] (a) C. Dass, *Mass Spectrom. Rev.* 9 (1990) 1; (b) F. Berruyer-Penaud, G. Bouchoux, *Rapid Commun. Mass Spectrom.* 4 (1990) 476; (c) P. Mourgues, C. Monteiro, H.E. Audier, S. Hammerum, *Org. Mass Spectrom.* 25 (1990) 389.
- [30] Calculations show that complex **4** probably could not be formed directly, because of a repulsive interaction between the hydroxylic hydrogen of methanol and the positively charged oxygen of ionized acetaldehyde.
- [31] Although the H<sub>6</sub>–O<sub>4</sub> distance is shorter in the transition state than in the precursor **4**, both structures were shown to be connected by slightly changing the H<sub>7</sub>–C<sub>1</sub> distance and optimizing for a minimum.
- [32]  $\Delta H_f$  [CH<sub>3</sub>COH<sup>+</sup>] = 199.4 kcal mol<sup>-1</sup> was evaluated from  $\Delta H_f$  [CH<sub>3</sub>CHO<sup>+</sup>] = 196.3 kcal mol<sup>-1</sup> [2] and its difference with  $\Delta H_f$  [CH<sub>3</sub>COH<sup>+</sup>] calculated at the G2 level [4].
- [33]  $\Delta H_f$  [CH<sub>2</sub>COH] = 21 kcal mol<sup>-1</sup> was evaluated from  $\Delta H_f$  [CH<sub>2</sub>CHOH] = -30 kcal mol<sup>-1</sup> and from the difference of  $\Delta H_f$  between C<sub>2</sub>H<sub>4</sub> and C<sub>2</sub>H<sub>3</sub> [2].